# Engineered Polypeptides as a Tool for Controlling Catalytic Active Janus Particles

*Marola W. Issa[1], Diego Calderon[2], Olivia Kamlet[1], Sogol Asaei[1], Julie N. Renner[1], and Christopher L. Wirth[1]*

*[1]Department of Chemical and Biomolecular Engineering, Case School of Engineering, Case Western Reserve University, Cleveland, Ohio 44106, United States*

*[2]Department of Biology, College of Arts and Sciences, Case Western Reserve University, Cleveland, Ohio 44106, United States*

**Corresponding author**

Christopher L. Wirth

Chemical and Biomolecular Engineering Department

Case School of Engineering

Case Western Reserve University

Cleveland, OH 44106

clw22@case.edu

MWI Orchid: 0000-0002-8099-0459

CLW Orchid: 0000-0003-3380-2029

JNR Orchid: 0000-0002-6140-4346

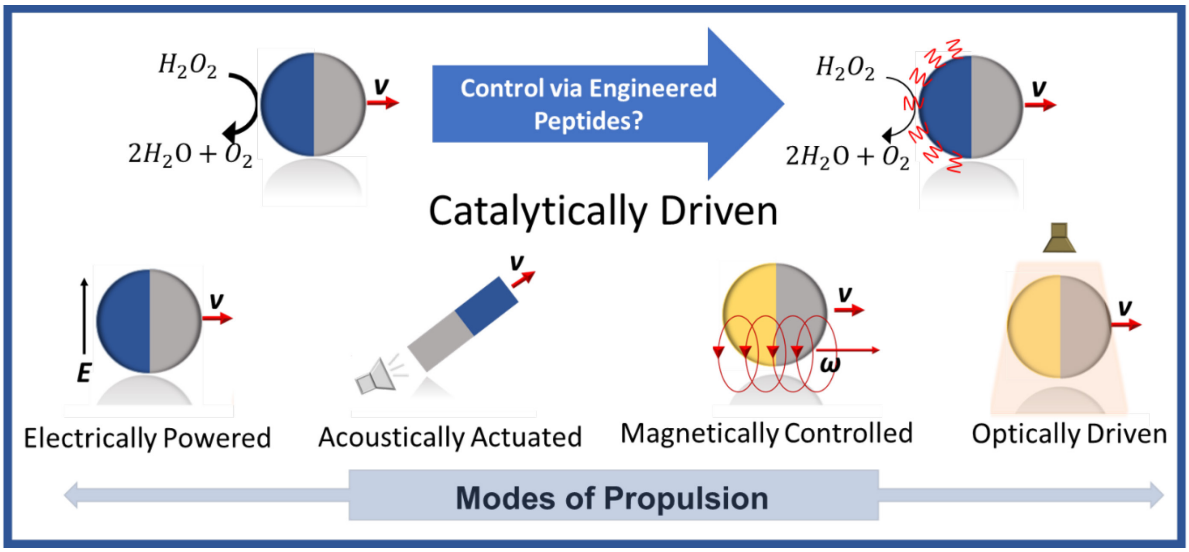
$H_2O_2$
$2H_2O + O_2$
v
Control via Engineered Peptides?
$H_2O_2$
$2H_2O + O_2$
v
Catalytically Driven
v
E
Electrically Powered
v
Acoustically Actuated
v
ω
Magnetically Controlled
v
Optically Driven
Modes of Propulsion

ABSTRACT

Active Janus colloids are functional particles that combine two distinct chemical or physical surface properties. The anisotropic nature of this class of patchy particles allows them to harvest and redirect energy to create a local force that leads to autonomous motion. Modulating the surface forces experienced by or the responsiveness of a Janus particle's surface offer an avenue of further control. There are broad efforts in the community to advance the fundamental understanding of and engineer such control into active systems. This article aims to summarize recent work in catalytic active Janus colloids, peptide and polypeptide engineering and design, and present work showing how engineered polypeptides can be used to control motion of catalytic active particles. Experiments probing non-specific effects are reviewed that measured the active motion of 5 μm catalytic Janus spheres in the presence of low molecular weight polyethylene glycol (PEG). Previous work has found that at infinitely dilute concentrations of particles, the addition of PEG in solution reduced particle propulsion speed. Further increasing particle concentration led to increased clustering at low concentrations of PEG, but clustering was then reduced at high concentrations of PEG. These results inspired work presented herein with 3 μm particles that shows platinum binding peptides that specifically attach to the platinum cap reduced the propulsion speed. These data support a pathway for using engineered peptides as tools for controlling the activity of catalytic active Janus particles. Overall, this article highlights how non-specific and specific molecular interactions can achieve control in active systems.

Keywords: Janus particles, peptide design, surface-functionalized micromotors, autonomous molecular control, active matter

## I. INTRODUCTION

Micrometer scale Janus colloids are chemically anisotropic particles that have garnered broad interest over the past two decades.[1–3] "Active" Janus colloids generate a mechanical force in response to environmental cues, which can be either locally or externally applied.[4–7] These systems undergo deterministic motion because of a break in symmetry, enabled by the patchy chemical morphology.[1] The synergism between environmental cues and the local break in symmetry actuates motion.[4,8,9] Environmental cues that induce a mechanical force include light, chemical reactions, acoustic, magnetic, electric fields, and even enzymatic driven reactions.[10–17] Ensembles of active Janus particles display a wide variety of intriguing individual (i.e., near interfaces) and collective (i.e., near neighboring particles) dynamics in response to local crowding.[18–22] These complex dynamics will often influence local assembly and bulk fluid properties.[23] Further, these phenomena allow active Janus particles to serve as analogs for microorganisms (i.e., multiflagellar bacteria), controlled cargo microscale transport, and biosensing.[24–28]

Early work in this area includes the fabrication of catalytic driven rod-shaped particles consisting of platinum and gold segments.[4] These particles were made active by introducing aqueous hydrogen peroxide ($H_2O_2$), which undergoes decomposition on the platinum segment. Further work on catalytic powered Janus spheres has since been extensively investigated.[29–32] The speed with which a catalytically active particle propels has been found to scale with the concentration of hydrogen peroxide, suggesting a mechanism that is reliant on that fuel.[33] The decomposition reaction associated with these catalytic active systems generates a concentration gradient that is thought to induce propulsion via distinct mechanisms dependent on the conductivity of the native particle. It is important to note, however, there is work suggesting the

origin of motion arises from different mechanisms. For instance, although many accounts attribute self-diffusiophoresis as the mechanism responsible for propulsion of a non-conductive particle with a platinum cap, other work suggests self-electrophoresis or electrokinetic effects in general is the dominant mechanism[34–36]. Work on catalytic driven colloids has further found an influence of cap surface morphology on particle dynamics.[37] Our own work contributed to this understanding by developing a technique for the direct measurement of cap thickness. The method utilized focused ion beam slicing and image analysis which enabled for local and direct measurements.[1]

In addition to chemical and physical pathways, applications of external fields have also been used to drive active particles. Field-induced propulsion includes motion in response to electric, magnetic, optical and acoustic fields.[38–40] External fields allow for precise control of the energy source and provide an advantage over catalytic driven systems where the fuel depletes over time. Optically powered systems are a subclass of field-driven colloids that have received considerable amount of interest.[41–44] In one example, nanoparticles with a plasmodium morphology were powered by light such that rotation of the asymmetric particles led to active motion.[45] This work allowed researchers to take advantage of the momentum of photons and to use it for inducing controlled rotational forces. Similar work on gold-capped silica spheres induced propulsion via self-thermophoresis.[44] Ultimately, when exposed to light, the conductive gold cap absorbed the laser with a particular intensity and heated up rapidly. The metal hemisphere then transferred heat to the surrounding liquid leading to a gradient in the local temperature that drove motion. Further, gold-capped, and graphite-capped silica spheres suspended in a binary liquid mixture were observed to propel via self-diffusiophoresis when illuminated by light.[42,46] Motion in this case was initiated by the illumination-borne heating which works to induce a local demixing

of the binary mixture. The asymmetric demixing generated a spatial chemical concentration gradient driving autonomous motion.

Magnetically powered micromotors have emerged as another fertile area of study in field-powered colloids. A central topic in this area is the study of particles that have the unique ability to harvest and redirect magnetic energy to generate localized hydrodynamic gradients. Further, the gradients lead to a break in symmetry which actuates autonomous motion. One such example is that of a flexible magnetic bead "tail" connected to a blood cell "head". When subjected to an oscillatory magnetic field, the self-assembled tails distorted the surrounding fluid leading to active locomotion.[13] Additional work included the fabrication of microrods "microkayaks" that undergo translational motion when actuated near a solid surface. Ultimately, when magnetized orthogonally along their axes, the microrods demonstrated a precessing motion allowing them to propel.[47] Another example is that of micromotors comprising a native helical structure with magnetic metal coatings on one end. When subjected to a rotating or an oscillating magnetic field, these micromotors experienced translational motion.[13,48,49]

Electric field powered micromotors are another subclass of field-driven colloids which have received a considerable amount of interest.[12,50–52] An example of this subfield included diode-based rotor rings actuated with an AC current.[53] Application of external AC fields allowed the diodes to acquire a break in symmetry and exhibit rotational motion. Semiconductor diode nanowires were also propelled in an AC field.[11] Ultimately, autonomous motion in this case was facilitated by the diodes' ability to rectify an AC signal and convert it to a localized DC field. Additional work demonstrated the ability to control the orientation and direction of these systems nearby an air-water interface.[11] Micromotors powered by external electric fields show promise for biomedical applications where propulsion can be induced by applications of very low field

strengths.[54] Further, in-vivo imaging and actuation of a swarm of magnetic helical microswimmers in deep tissue have been domonstrated.[26] Notably, multi-stimulus-responsive particles represent exciting advancements with diverse transport modes. Polymer-based micromotors powered by various chemical and physical stimuli exhibit versatile on-off-on motion and directional navigation.[45]

As summarized above, there has been a substantial depth and breadth of work exploring the complex behavior of active systems. A wealth of effort has been invested in understanding and then subsequently engineering forces that aim to guide dynamic behavior. One emerging area in this effort is that of control via molecular modifications of active systems. Molecular control of active systems could potentially be used to achieve modulation of both conservative (i.e., path-independent) and non-conservative (i.e., path-dependent) interactions. Recent efforts to tune particle dynamics resulted in the functionalization of gold-platinum (Au-Pt) bimetallic micromotors with a thermoresponsive polymer chain. The conformation of the polymer brush enabled directional navigation.[55] There was a complementary effort aimed to probe Janus particle dynamics near a functionalized boundary.[56] The polymer conformational reconfiguration in response to temperature enabled the tuning of propulsion speed. Autonomous micromotors for biomedical applications necessitate the design of compatible polymers. For instance engineered polypeptides may offer an advantage because of their enhanced biodegradation, high biocompatibility, tunability, multifunctionality, and responsiveness to external cues.[57] Herein, we aim to spotlight work that suggests engineered polypeptides offer significant opportunity in this respect.

This manuscript aims to highlight work in engineered stimuli-responsive polypeptides and the opportunities for using these materials to control catalytic active particles (see **Figure 1**). In

addition to summarizing these fields, we also present new experiments that capitalize on newly designed peptides with platinum binding tags. Experiments were conducted to measure the influence of decorating a catalytic active particle with these polypeptides demonstrated to have high affinity for platinum materials. We found these platinum-binding peptides to influence the motion of 3 μm catalytic Janus spheres to an extent like that of previous work conducted with low molecular weight polyethylene glycol (PEG). Note that although there is a substantial volume of work in active and driven systems to which this framework could be applied, herein we focus on catalytic active Janus particles. The previous and new work summarized here provides a prospective on an emerging opportunity in molecular control of active systems via tuning both specific and non-specific interactions.

## 2. THEORY AND ANALYSIS OF CATALYTIC ACTIVE SYSTEMS

*a. Mechanism and analysis framework for propulsion.* Catalytic powered Janus colloids perform autonomous propulsion in response to a chemical reaction. Namely, platinum acts as a catalyst to decompose the hydrogen peroxide "fuel" in solution. The catalytic decomposition of fuel (i.e., $H_2O_2$) forms a gradient in solute molecules (electrolyte and non-electrolyte) on the length scale of the particle. This leads to generation of a slip velocity along the particle surface that is thought to actuate self-diffusiophoresis. As noted above, there remains debate in the community concerning the mechanism and it is thought for example the nature of the particle itself may lead to additional effects. For instance, a particle consisting of two conductive materials, for example gold and platinum, will experience self-electrophoresis at some conditions.[5,58] This mechanism is relevant when there is charge transfer between the two materials and an associated electric field generated in the vicinity of the particle.

Despite the substantial work over the past two decades on the general mechanism by which propulsion occurs, there are considerably fewer studies on the chemical pathways, kinetics, or molecular control of these mechanisms within the context of catalytic active Janus particles.[35] Given the complexity of platinum catalyzed hydrogen peroxide decomposition and the potential to control the associated kinetics, this is one area in which we feel additional work is justified. Further, these chemical transformations induce changes in surface chemistry. Particles regularly interact with surfaces via conservative and non-conservative interactions. Conservative surface interactions typically depend on physiochemical properties including suspension pH, particle charge and concentration. Non-conservative interactions arise from active particle shape or geometric confinement. The complex interplay between physiochemical and hydrodynamic forces greatly influences particle dynamics. Ultimately, these interactions provide an avenue for control of the active motion.

The motion experienced by an active particle consists of a superposition of stochastic "Brownian" fluctuations and deterministic motion. A typical experiment aimed at measuring the deterministic velocity consists of tracking the trajectories of individual particles and then calculating the mean squared displacement (MSD) from those trajectories. A recent perspective provides a detailed and practical guide to the appropriate analysis framework for active systems.[59] The particle activity is then inferred from the propulsion speed, which is obtained from a fit of the MSD, $<r^2>$. In the absence of fuel, the particles are considered "passive" and the MSD associated with their stochastic fluctuations due to thermal agitations is depicted by Eqn. (1). Upon the addition of fuel, the general MSD associated with individual Janus particles is depicted in Eqn. (2).[33] Note that Eqn. (2) is the general expression used for all conditions, whereas there are limiting forms of the expression that are typically implemented.

$$< r^2 > = 4\, D_0 \tau \quad (1)$$

$$< r^2 > = 4\, D_0 \tau + \frac{v_p^2\, \tau^2}{2}\left[\frac{2\tau}{\tau_r} + e^{-2\tau/\tau_r} - 1\right] \quad (2)$$

Above, $D_0$ is the diffusion coefficient, which is obtained by fitting the MSD trajectories, $\tau$ is lag time, $\tau_r$ is the rotational diffusion time, and $v_p$is the apparent deterministic speed. In the case of particles in the absence of fuel, Eqn. (1) can be used to fit an MSD that is linear in lag time with a slope equal to 4 $D_0$. This process is often used in microrheology experiments to obtain $D_0$ and then viscosity in cases where the probe size is known. MSD data obtained for catalytic active Janus particles is fit with Eqn. (2), which is parabolic in lag time, $< r^2 > \approx 4\, D_0 \tau + v_p^2\, \tau^2$, when that time is much shorter than the rotational diffusion time, $\tau << \tau_r$. Experiments conducted in our lab with particles that have a diameter ≥ 3 μm reside in that regime because the $\tau_r$ is on the order of 10 seconds. From these fits, one can obtain the apparent speed and then report that value for systematic changes in some experimental condition. Other analyses include tracking the shape of trajectories or the proximity of those trajectories to boundaries.[60]

Ensemble behavior is also of great interest to those conducting active particle experiments as it elucidates the way in which the interactions among individual particles collectively impact the behavior of the system. Gaining insights into this collective behavior can lead to a better understanding of emergent phenomena including pattern formation, synchronization, and phase transitions that cannot be accounted for otherwise. Furthermore, the behavior of an ensemble of active particles can impact the overall functionality and performance of the system, such as its ability to navigate and self-assemble. Hence, investigating an ensemble of active particles is crucial for practical applications in fields such as drug delivery. One such behavior that is measurable is that of clustering dynamics. One strategy of extracting cluster information is to measure the population balance of clusters as they evolve in time. Imaging processing has been used to track

the quantity of clusters from each population to evaluate whether living crystals have been formed or growth of a cluster continues in an unbounded fashion. In our previous work,[10] we tracked cluster formation by measuring the number of objects of a given population (doublets, triplets, etc…) in the entire ensemble. This measurement provided the fraction of a given population or % Observed. Larger values of % Observed for a given classification indicates a larger fraction of particles belonging to that class. % Observed was calculated via the following equation (Eqn. (3)).

$$\% \, Observed = \frac{N_i}{\sum_{i=1}^{3} N_i} \tag{3}$$

$N_i$ represented the number of objects observed of each of the three classifications. For example, (i=1) refers to singlets, (i=2) intermediates, and (i=3) for clusters. For cases in which colloidal crystal growth occurs, these quantities increase and decrease as larger crystals form. For instance, the intermediate % observed will initially grow as doublets form, but then that population will decrease as those doublets become triplets, 4-mers, 5-mers, etc.. However, in cases that living crystals form, which is when there is a pseudo-equilibrium size of crystals, a given population will grow to a stable % Observed value. Note there are other also useful measures of ensemble behavior for active systems, including measures of structure factor and/or nearest neighbor.[61]

*b. Particles close to neighbors and boundaries.* Micrometer scale colloidal particles regularly interact with boundaries via both conservative (path-independent) and non-conservative (path-dependent) interactions. Path independent conservative interactions typically depend on surface chemistry of the boundaries and bulk, for instance if the particle and nearby substrate are negatively charged or the concentration of electrolyte in solution. Conservative interactions such as repulsion caused by the overlap of similarly charged electric double layers associated with each boundary, van der Waals attraction, or depletion attraction caused by non-adsorbing nanoparticles or polymers have previously been measured.[62–66] Path dependent conservative interactions, for the

most part hydrodynamic interactions, are also influenced by physiochemical properties, such as fluid viscosity, but are additionally influenced by system-specific factors, such as the rate and orientation of the particle as it approaches the boundary. These phenomena have also been measured for non-active systems, with a growing appreciation over the last decade of how such phenomena may play a role in the dynamics of active systems.

As with non-active particles, catalytic active particles will interact with neighbors and nearby boundaries with conservative and non-conservative interactions. These interactions are affected by not only the presence of the non-uniform distribution of solute in the particle vicinity, but also the superposition of both stochastic and deterministic motion characteristic of an active particle. Perhaps the most striking effect is that of clustering experienced by ensembles of active particles. Active particles, both those driven by demixing and those driven by a catalytic reaction, have been observed to form "living crystal" clusters at sufficiently large number concentration and larger crystals at concentrations above the living crystal regime.[61]

A simplified explanation for clustering considers the process of particle collision followed by reorientation.[67] Upon a collision, the deterministic motion of two or more particles will be halted such that a small cluster is formed. The cluster will remain until enough time passes for one or more of the particles making up the cluster re-orients to propel away. Production of living crystals would then be dictated by the speed with which individual particles propel and the number density of the ensemble. Continued crystal growth occurs with a sufficiently small mean collision time, which is impacted by both the propulsion speed and number density of particles. A similar process unfolds when active particles approach boundaries. Active particles will sample boundaries with a set of outcomes (ex. repulsion or attraction) depending on conditions related to orientation and cap coverage.[68,69] Experimentally, particles have most often been observed to stay

near a boundary. One such example was that of a catalytic active Janus particle that was observed to approach and closely follow a corner geometry.[70] The authors attributed this behavior to the physical reorientation mechanism mentioned above. Other work has also revealed the importance of a chemotactic influence, or how the nearby boundary impacts the chemical field surrounding the particle to the extent the particle is retained close to the boundary.[68]

## 3. DESIGNING PEPTIDES AND POLYPEPTIDES

*a. Peptide and polypeptide engineering and design.* Polypeptides are chains of amino acids linked together by covalent peptide bonds, formed by a condensation reaction between an amino group of one amino acid, and a carboxylic acid group of another amino acid. Each amino acid has a unique side chain. There are 20 natural amino acids which span a range of properties dictated by their side chain, including varying hydrophobicity, pKa, polarity and reactivity. **Fig. 2(a)** shows an amino acid with the side chain designated by R as well as the amino and carboxylic acid groups highlighted. The order of the amino acids in the chain is known as the primary sequence. Primary sequences give rise to the next level of polypeptide structure known as secondary structure, which is the local folded structures that form within a polypeptide and include structures like α-helices and β-sheets. Secondary structure gives rise to tertiary structure, the overall three-dimensional structure of the polypeptide, and tertiary structures can combine to form quaternary structures. **Fig. 2(b)** shows the different levels of polypeptide structure. Techniques to assess polypeptide sequence, size, and structure include liquid chromatography with tandem mass spectrometry, polyacrylamide gel electrophoresis, circular dichroism, nuclear magnetic resonance, and infrared spectroscopy.

Longer polypeptides that arrange into biologically functional constructs are called proteins. Shorter chains containing less than 50 amino acids are called peptides. Polypeptide engineering is

the process of developing polypeptides for a specific valuable function, and has resulted the development of new biomaterials,[71] drug-delivery platforms,[72,73] therapeutics,[74] antimicrobial agents,[75] nanomaterials,[76] hydrogels,[77,78] electrochemical systems,[79] sensors,[80] and superior biocatalysts.[81,82] Benefits of polypeptide engineering include the ability to specifically and easily define and tune the sequence of amino acids in a polypeptide chain, where in addition to natural amino acids unnatural amino acids can also be incorporated into the sequence, expanding the available design space.[83,84] Other benefits of polypeptide engineering include biocompatibility as well the ability to design multiple functions[85] and stimuli-responsiveness[57] into the molecules. Polypeptides are also easy to manufacture using established molecular biology techniques where the DNA of a host organism is strategically manipulated such that the organism will produce the polypeptide of interest. Techniques to manufacture polypeptides on the commercial scale are well-established.[86] For shorter peptide sequences, synthetic approaches have also become feasible at large scale,[87] and conducive to fast turnaround times for laboratory testing. Strategies for determining the sequence of polypeptide include directed evolution,[88,89] rational design and semi-rational design,[90] as well as de novo design.[91] Computational methods, as well as machine learning have are also utilized in the design process.[92,93] In addition, modular designs and biomimetic approaches have been utilized to develop multifunctional polypeptide materials.[94] Often, combinations of these techniques are utilized to achieve the a polypeptide design, and iterations testing and redesign are also executed as part of the process.

*b. Affinity sequences.* One advantage of peptides and polypeptides is their capacity for biorecognition. Sequences that can selectively bind to targets have been utilized for drug delivery,[95] nanomaterial assembly,[96] biosensing,[97] and protein purification.[98] Depending on the application, sequences that have already been discovered to have high affinity for a target can be

utilized, iterated, or newly designed.[99] There is an opportunity in the active Janus particle community to utilize polypeptide specificity for biological targets, as well as utilize polypeptide affinity for solid materials including gold[100] and platinum.[101] For example, peptide-functionalized gold nanoparticles already serve as effective cell-targeting agents.[102] In addition, peptides bound to solid surfaces have been shown to influence catalytic reactivity in various ways, including via controlling surface coverage and stabilizing catalyst composition (**Fig. 3**).[103,104] In one illustrative example, a series of gold-binding peptides were used to make gold nanoparticles and it was discovered that the aspects of the biotic/abiotic interface including the amount of exposed gold surface, the underling surface structural disorder, and the interaction strength of the peptide all influenced the catalytic activity of the materials for 4-nitrophenol reduction.[105] Examples of controlling platinum reactivity via peptides have also been reported.[101] Affinity is assessed using techniques such as isothermal calorimetry, surface plasmon resonance, and quartz crystal microbalance with dissipation monitoring.

*c. Stimuli responsiveness*. Another highly attractive feature of engineered polypeptides is the ability to render them stimuli-responsive. Thorough reviews have been composed on amino acid-derived stimuli-responsive polymers,[106–108] with a plethora of stimuli including light, temperature, pH, redox state, ion binding, gas, and biochemical entities (**Fig. 4**). These materials change structure and thus function upon exposure to one of these stimuli. Stimuli-responsive polypeptides have found use in drug-delivery[57] and biomedicine[109] including biomaterials for wound healing,[110] and cancer treatment[111] among many others. Stimuli-responsive peptides have also been utilized to modulate the reactivity of catalytic surfaces.[112–115] By incorporating a non-natural amino acid containing azobenzene, the configuration of a peptide can be switched because azobenzene assumes a cis configuration when exposed to UV light, and a trans configuration when exposed to

white light. Surface-bound peptides containing an azobenzene moiety have been demonstrated to modulate the amount of catalytic surface covered by the peptides, and thus modulate reactivity. For example, optical control of the reduction of 4-nitrophenol on gold nanoparticles capped with photosensitive peptides has been previously demonstrated.[112]

## 4. CONTROL VIA NON-SPECIFIC INTERACTIONS

For the purposes of this article, we consider non-specific interactions to be those related to environmental geometry or continuous phase chemistry that may lead to a surface interaction, such as depletion attraction. The past decade has seen significant effort in utilizing such cues to control active Janus particles. Active particles interact with boundaries in complex ways, with a variety of factors influencing the retention or repulsion of those particles to or away from the boundary, respectively. There are excellent examples exploring how active particles sample the topography of a substrate or the space within porous media, with most experimental work finding that active particles tend to be retained to boundaries and follow the contour of corners. These observations are particularly notable because of its common features with biology. Entities in biology that are known to self-propel (ex. microorganisms) are regularly found near boundaries.[116] As such, synthetic active particles serve as an excellent model system for exploring the complex dynamics leading to these behaviors found in nature.

One early example of how catalytic active particles sample topography showed the persistent motion of particles along boundaries of varied shape.[117] Micrometer scale Janus particles were prepared with a base silica sphere and a thin platinum cap covering approximately one hemisphere of the particle. The particles were initially suspended in water, absent of hydrogen peroxide “fuel”, in a fluid cell with a substrate of varying topography, including corners, steps, and circular posts. Initially, the authors found the Janus particle to be sampling orientations with

the cap facing downward, likely a result of gravitational quenching.[117] Once hydrogen peroxide was added, the Janus particle reoriented with the boundary between the Janus cap and base particle perpendicular to the substrate. Propulsion of the Janus particle then commenced with its trajectory tending to be trapped or follow along a corner feature. This behavior was further explored by tracking the approach of a Janus particle to a boundary with systematic variations in height between 4% and 80% of the particle's radius (see **Fig. 5**). They found that Janus particles were unlikely to pass steps with a height just 8% of the largest particle's radius, demonstrating that even small topographical features can capture particles. Once trapped, these particles tended to reorient and track along the corner feature. The tracking behavior persisted regardless of the curvature of the corner. For example, the catalytic active Janus particles followed a path tracing the perimeter of the circular post. Tracking behavior tended to persist longer at larger fuel concentrations. The authors attributed these behaviors to a combination of hydrodynamic interactions and the chemical activity of the catalytic Janus particle.

Experiments with the same goal, to understand how catalytic active Janus particles are retained to surfaces, were conducted with a substrate of varied pseudo 3D topography created by a colloidal crystal.[118] Catalytic active Janus particles were tracked in a colloidal crystal to obtain the frequency with which an active particle hopped from one particle in the crystal to another ("hopping rate"). Like the work described above, the authors found the hopping rate decreased with increasing hydrogen peroxide concentration (i.e., active particles were more likely to persist on a track along a corner with increased fuel concentration). Surprisingly, these experiments also revealed only a weak to nil dependence of the hopping rate on speed. These data at minimum suggest a combined influence of both hydrodynamics and chemotactic influence in trapping but could be extrapolated to assume only chemical activity is responsible for trapping a Janus particle

near a boundary. Complementary experiments were performed with *E. Coli* showing the microorganism tended to propel in straight trajectories through the interstitial spaces of the colloidal crystal. This dramatically different behavior was attributed to the inability of a microorganism to reorient upon interaction with a boundary. These excellent examples have been followed by others that revealed a combined impact of hydrodynamic and chemical interactions.[119]

Control of catalytic active Janus particles has also been achieved via addition of solutes or dispersed material that modify the local chemical cues experienced by a particle. Some of the earliest examples of this work observed that the addition of salt or surfactant could effectively reduce the propulsion speed of a catalytic active Janus particle consisting of a polystyrene bead and platinum cap.[34] The addition of neutral salts (NaCl and KBr) reduced propulsion speeds from approximately 15 μm/s to ~0 μm/s at a concentration of 1 mM. The authors further found the addition of an anionic surfactant, cetrimonium bromide (CTAB), to quench propulsion speed even more dramatically. The authors suggest that these effects could be explained by previously unaccounted for currents flowing internal to the platinum cap and ultimately that self-electrophoresis is the dominant mechanism responsible for propulsion.[35] Variations in cap thickness or local nonuniform concentration of the $H_2O_2$ may contribute to currents within the conductive platinum.

Over the past four years, our group has had a developing interest in the control of catalytic active Janus particles proximate to boundaries. We explored how surface interactions could be adjusted to impact apparent speed or clustering behavior. Initial published work aimed to control active Janus particles consisting of 5 μm platinum-coated polystyrene spheres at infinite particle dilution (far from neighbors) and in hydrogen peroxide.[9] Control experiments showed the apparent speed increased roughly linearly with increasing hydrogen peroxide concentration (see **Fig. 6**).

Following the control experiments, dispersed nanomaterials were added and the impact on speed was measured. Two separate experiments were conducted, namely one with charged 20 nm sulfate-modified polystyrene particles dispersed among the active particles and a second with uncharged PEG of molecular weight ~6000 g/mol. Particle speed decreased by increasing the depletant volume fraction and decreasing fluid conductivity (see **Fig. 6**). These data suggested the addition of dispersed nanomaterial (either nanoparticles or PEG) reduced the propulsion speed via synergetic influence of hydrodynamic hinderance in response to depletion attractions as the particles are pulled closer to the boundary and suspension conductivity.

Previous work had shown that ensembles of active particles propelling via a non-catalytic mechanism displayed dynamic clustering behavior dependent on speed and number concentration.[42] The authors attributed the clustering behavior to the interplay of hydrodynamic and the finite time scales associated with reorientation of the clustered particles. Further, interactions with nearby boundaries and between neighboring particles strongly influence dynamics. Our group further explored this phenomenon by probing the influence of PEG on the collective behavior of catalytic active Janus particles.[10] We measured the effect of PEG on this clustering behavior in catalytic active particle systems at intermediate particle concentration.

At suitable number concentrations, the active particles displayed small cluster formation with dynamic exchange (i.e., living crystals) between singlets and intermediates (see **Fig. 7**). The extent of clustering grew as a function of increased activity modulated by peroxide concentrations. Subjecting the ensemble to dispersed material, namely the PEG utilized in our earlier work, revealed a decrease in clustering at intermediate to high PEG concentrations. This was attributed to the reduction in speed we observed earlier. Surprisingly, we found that at low PEG concentrations, the clustering phenomena was enhanced. In this regime, PEG did not change

collision probability and produced no change in particle speed. However, once collision occurred, we hypothesized that PEG enhanced the attractive particle-particle interactions via depletion. As PEG concentration was increased, the propulsion speed decreased thereby decreasing the probability of collision and cluster formation (see **Fig. 7**). Note these and the other experiments described used a glass slide as a substrate. Given the apparent importance of conservative surface interactions experienced by a catalytically active particle with a nearby substrate, one might expect the nature of the substrate to play a role on the propulsion of catalytically active particles.

## 5. MATERIALS AND METHODS

New experiments were conducted to evaluate whether engineered peptides could be used to control propulsion of catalytic active particles.

*a. Fabrication of Janus particles and assembly of experimental fluid cell*. Catalytic active particles are typically visualized with a light microscope in a fluid cell, but there is one other excellent example in which light scattering was used to track activity.[120] Previously published and new experiments described in this article were conducted with light microscopy. Polystyrene beads with nominally 3 μm diameter were obtained from Fisher Scientific (Lot #2307860). Platinum coated polystyrene Janus spheres were prepared similarly to the method described in our previous work.[9] Briefly, the substrates comprising 20 x 20 mm silicon wafers were first made hydrophilic via plasma cleaner. Next, a monolayer of polystyrene spheres was deposited onto each wafer via a spin coater operated at 6000 revolutions per minute (RPM). Polystyrene-platinum (PS-Pt) Janus microspheres were then prepared by depositing ~ 20 nm platinum on the polystyrene monolayers using physical vapor deposition. Following the fabrication process, ultra-sonication was used to resuspend the Janus spheres in ultra-pure water. Lastly, the suspension was washed three times by centrifugation and supernatant exchange.

Fluid cells were assembled by attaching a secure-seal spacer gasket (Fisher Scientific) with a circular available area that had a 7 μL volume and 9 mm diameter to a microscope slide that had been previously rinsed with isopropanol and ultra-pure water. Once the sample was loaded, the cell was quickly capped with a glass cover slip to minimize evaporation. Video capture was carried out immediately following cell assembly. All videos were collected at a rate of 10 frames per second (FPS) with exposure time of ~ 100 ms. Each experimental video was analyzed with a standard particle tracking algorithm[121,122] executed in MATLAB for apparent speed measurements.

*b. Peptide design, synthesis, and impact on local chemical environment*. The proposed framework, which involves the design of peptides to regulate the propulsion of catalytic active Janus particles, should be complemented by techniques to deduce the effect of these materials on the catalytic reaction that takes place on the platinum cap. Peptides offer a material platform with specific affinity to substances used in active systems and can also be engineered to respond to external cues. This platinum affinity peptides were designed based on work by Seker *et al.* (l-PtBP1: CPTSTGQAC and l-PtBP2: CQSVTSTKC) in linear form.[123] Linear forms of the peptides were chosen because of their intermediate binding affinity estimated to be 0.16 X $10^6$ $M^{-1}$ $K_{eq}$ for both peptides. No modifications were made to the N- or C-terminus of 1-PtBP1 or 1-PtBP2. A control peptide was designed to have low affinity for platinum based on work by Pramounmat *et al.* (Non-PtBP: Ac-CVPGVG-$NH_2$).[124] All three peptide sequences were synthesized by GenScript and arrived in lyophilized powder form at a purity of ≥95%.

*c. Peptide incubation with Janus particles.* For the PtBPn (platinum binding-polypeptide, where n = 1,2) to bind to the Pt-PS Janus particles, the polypeptides and the particles were incubated together. A suspension of Pt-PS particles in ultra-pure water (1.5 mL) was prepared in

a 1.5 mL centrifuge tube. The amount of Janus particles in the suspension was approximately equal to the amount of Janus particles covering ⅛ of the area of a 20 mm x 20 mm silicon wafer when it was created. The tube was centrifuged for 5 minutes at 4,000 revolutions per minute (rpm) or 1500g Relative Centrifugal Force (RCF). Once it was confirmed that the Pt-PS particles adhered to the side of the centrifuge tube, using a pipette, as much of the supernatant water were removed as possible from the tube without disturbing the adhered particles. The x μg/mL PtBPn solution (1 mL, where x = 2.5, 5, 10) was added to the centrifuge tube with the Janus particles adhered to the side. The centrifuge tube was then sonicated for a minute and vortex mixed to ensure the Janus particles separated from the side of the centrifuge tube. The tube was placed into a centrifuge and allowed to incubate for 20 minutes at 25°C before the centrifuge was turned on. The tube was centrifuged for 5 minutes at 4,000 rpm or 1500g RCF. To remove excess, unbound polypeptide, the supernatant was removed with a pipette and an equal volume of DI water was replaced into the tube. The tube was centrifuged again for 5 minutes at 4,000 rpm or 1500g RCF and the supernatant was removed twice more, for a total of three times.

*d. Quartz crystal microbalance with dissipation monitoring*. The adsorption of the platinum-binding peptide with time was characterized by a quartz crystal microbalance with dissipation monitoring (Biolin Scientific, Q-Sense Explorer) in a standard flow module (nanoscience Instruments QFM 401). Platinum-coated sensors (QSX 314, nanoscience Instruments) were cleaned by UV/ozone treatment for 10 min followed by exposure to a hot (75°C) solution of 5:1:1 DI water, 25% ammonia and 30% hydrogen peroxide for 5 min. Sensors were rinsed again in DI water followed by another UV/ozone treatment for 10 min prior to use. Detailed protocols for module cleaning, and data analysis can be found in previous work.[125] Briefly, 10 μg/mL of each peptide was prepared in DI water. DI water was used as the baseline for the experiments and

solutions were flowed past the sensor at 0.150 mL/min a temperature of 18°C. After the frequency and dissipation signals of the baseline reached a stable value for 10 min, peptide solution was exposed to the platinum-coated sensor. Assembly was allowed to continue for ~3000 seconds. At ~3300 seconds, a rinse step was employed using DI water. The recorded data containing dissipation and frequency shifts were processed by QSense software, and the 9th overtone was selected for further analysis. Since the dissipation was sufficiently low, frequency was directly proportional to hydrated mass accumulated on the sensor and mass could be estimated using the Sauerbrey equation.[126] Estimates of hydrated mass were generated for each peptide using the average of the last two minutes of frequency data during the rinse step.

## 6. CONTROL VIA MOLECULES WITH SPECIFIC INTERACTIONS

Here, we consider specific interactions to be those interactions that are designed, via the choice of material chemistry, surface modification, or some specific interaction. Recently, there have been a number of contributions in this area.[55,127–129] Surface functionalization of the cap and/or base particle hemisphere with macromolecules that have a specific interaction has recently developed as a strategy for control of active systems. In one example, poly(N-isopropylacrylamide) (PNIPAM) was grafted onto the gold side of a gold/platinum capped Janus particle.[55] The PNIPAM has an experimentally accessible lower critical solution temperature (LCST), such that polymer chains extend into solution below that temperature and collapse to the substrate above the LCST. Janus particles were tracked, and the nominal propulsion velocity (both magnitude and directionality) was obtained in a solution of hydrogen peroxide above and below the LCST. The authors found that below the LCST (with PNIPAM fully extended) particles propelled in the direction of the platinum cap. Propulsion in the direction of the platinum cap (or a platinum/gold Janus particle) is consistent with a mechanism of self-electrophoresis, which

typically requires a Janus particle consisting of two conductive materials. When the temperature was increased beyond the LCST, the direction of propulsion was reversed, and the speed reduced. The authors attributed this behavior to a reduction of surface conduction between the gold and platinum regions because of the collapse of the PNIPAM to the surface of the gold. In addition, the authors found the grafting density played an important role in the efficacy of the control mechanism. Particles with a low grafting density of PNIPAM propelled in the direction of platinum regardless of temperature, while the effect of temperature was more pronounced as grafting density increased.

Our own emerging work has focused on the design of peptides with an affinity for platinum to specifically bind with the cap of an active Janus particle. As described above, there are several features of peptides that make them potentially useful to the control of active particles. Namely, these materials can be designed with specific sequences that attach to the different components employed in active particle systems, while peptides can be engineered to react to external stimuli, including temperature or electric fields. Below, we present new work in which we designed peptides to bind to the platinum and measured the influence of this coating on active particle speed.

First, we used QCM-D to verify that the designed peptides adsorb to platinum and to estimate the size and hydrated mass loading of the adsorbed layer. **Figure 8** shows the frequency and dissipation shifts with time for l-PtBP1 and 1-PtBP2. Once the platinum-coated QCM-D sensors were exposed to the peptide solution, a sharp decrease in frequency was observed for both peptides, indicating the peptides adsorbed to the surface. Upon rinsing with DI water, there was a small positive shift in frequency (less than 1 Hz) indicating the peptides were not easily rinsed away. The dissipation shifts for both peptides are low compared to frequency shift allowing the use of the Sauerbrey equation to estimate hydrated mass loading after the rinse step to be ~190 and

~160 ng/cm$^2$ for l-PtBP1 and 1-PtBP2, respectively.[130] As done in our previous studies with low dissipation thin layers of peptide,[125] assuming a density of 1100 g/L for hydrated protein allows the thickness of the hydrated layers to be estimated as ~1.9 and 1.6 nm or l-PtBP1 and 1-PtBP2, respectively. Our past work has shown good agreement between QCM-D estimated thicknesses and independent techniques such as ellipsometry.[131,132] These data indicate l-PtBP1 and 1-PtBP2 are likely adsorbed to the platinum surface of the Janus particles used in the following experiments that are meant to quantify the impact of platinum binding peptides on Janus particle speed.

To evaluate the impact of engineered peptide on the active system, we first measured the apparent speed of active Janus particles in 3% $H_2O_2$ in the absence of peptide as control. As with previous work, we tracked many particles, obtained trajectories, and calculated the MSD for each particle. Those measures of MSD were then fit with a model to obtain the apparent speed. We found the average apparent speed of the control group (~30 particles) to be ~ 1.3 μm/s (see **Fig. 9**). Variations in propulsion speed are expected because of small non-uniformities in particle size and cap quality inherent to the particle sample. Such variations are known to impact the propulsion speed and contribute to the large error bars.

A second control experiment was conducted that incorporated a peptide previously shown to have low binding affinity for platinum (named non-PtBP). The non-platinum binding peptides were incubated along with the Janus particle suspension and then washed before exposing those particles to hydrogen peroxide. In principle, all peptides should have been removed from the suspension with none specifically binding to the platinum cap. Statistical analysis was conducted on the data found in **Fig. 9**. Since normality and constant variance could not be assumed with this data set, a Kruskal-Wallis test was performed and it was found that the presence or incubation concentration of peptide caused a significant difference in speed. Next, a Dunn post-hoc test was

conducted where groups not sharing a letter (A or B) above their bars were found to be significantly different. Specifically, it was found that no peptide, and non-Pt binding peptide significantly different from all samples except PtBP1 at 2.5 μg/mL. There was no evidence that no peptide, and non-Pt binding peptide groups were significantly different. A family α value of 0.025 was used.

Functionalizing the Janus spheres with platinum binding peptides showed a statistically significant reduction in the average velocity compared to the non-platinum binding peptide control, and no peptide control (see **Fig. 9**). The reduction in average velocity compared to the controls was the same for both l-PtBP1 and l-PtBP2. This was expected considering the binding affinities of l-PtBP1 and l-PtBP2 to platinum were previously found to be similar.[123] We attribute the reduction in the measured apparent speed to the decrease in surface area available for the chemical decomposition to take place which led to a reduction in force generated by the particle. Although the propulsion data at 2.5 μg/ml peptide shown in **Figure 9** suggests saturation or perhaps even a sufficiently high coverage in which the peptide mitigates the catalytic reaction, it is difficult to extrapolate this conclusion from our QCM-D data. There are notable differences between the two experiments. Namely, the equilibrium coverage at 10 μg/ml bulk concentration in QCM-D is not necessarily equal to the equilibrium coverage at 2.5 μg/ml bulk concentration in the experiments with particles. In addition, coverage could be impacted by differences in platinum composition and the curvature of the particles. Additional experiments and a more detailed surface adsorption analysis would be required to determine the peptide coverage and saturation coverage on the platinum cap of the Janus particles used in the experiments summarized in **Figure 9**.

These data suggest the velocity of an active Janus particle is influenced by the available surface area of its catalytic side. To the best of our knowledge, these data are the first example of an engineered peptide being used to control the speed of a catalytic active particle. We aim for

these data to serve as the first step in designing systems with additional functions that offer more control of active particle systems. For example, there are published studies illustrating how to tune these sequences for a range of platinum affinity,[123] understand binding on a molecular level using molecular dynamics,[133] and design platinum-binding peptides for stimuli responsiveness.[134] While this peptide system only serves as an example, it illustrates that harnessing the established literature on engineered peptides and polypeptides will serve as a fruitful tool to control and study active Janus particles.

## 7. OUTLOOK AND CONCLUSIONS

This contribution aimed to both provide context for and show early data suggesting that engineered peptides can be used to control catalytic active Janus particles. As has been shown in other fields and technologies, these materials have the potential to specifically adsorb to surfaces and respond to stimuli. We presented a continuum of published and new work that illustrates how active particle systems can be controlled via non-specific and specific interactions. We conclude from our newest data that engineered peptides are a good tool for control of catalytic active systems. Our team sees integration of attractive engineered peptide features with active systems as the most fruitful near-term work for our community.

FIGURES

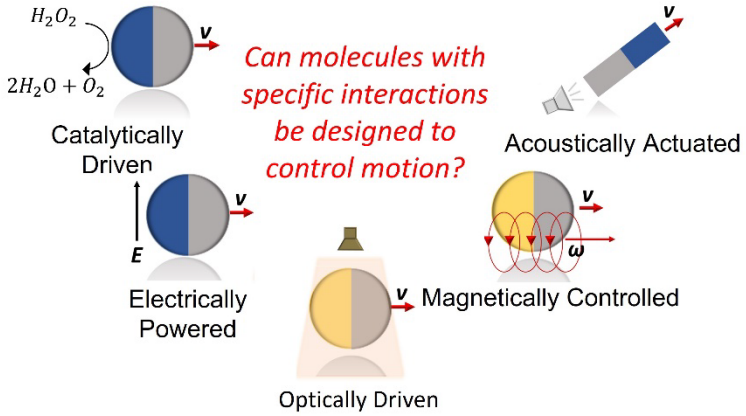


**Figure 1: Active systems that can benefit from molecular control.** Motion of micrometer scale Janus particles is actuated through internal or external fields, including the addition of fuel, electric, and magnetic fields. A key emerging question in this field is how to design molecular scale interactions to control motion.

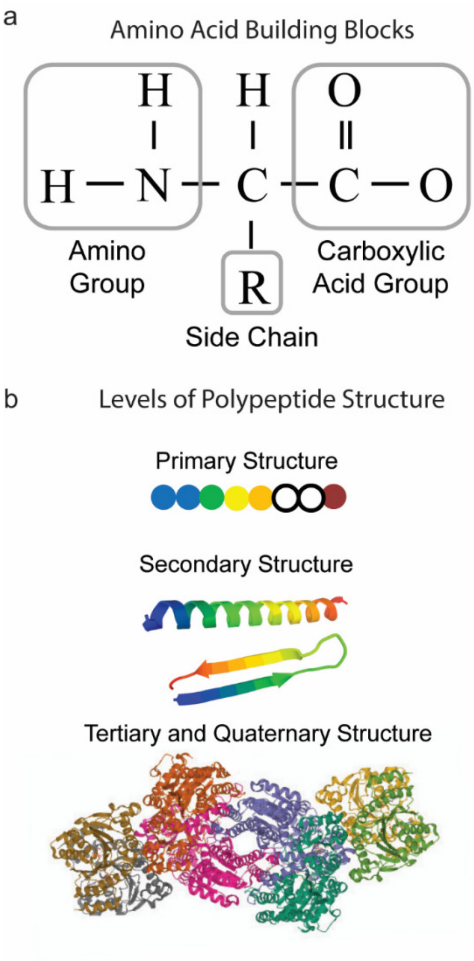


**Figure 2:** Polypeptide engineering involves developing polypeptide sequences for specific and valuable functions. Polypeptides are chains of (a) amino acids, which form by a condensation reaction between the amino group of one amino acid, and the carboxylic acid group of another amino acid. Each amino acid has a unique side chain, designated by 'R'. Polypeptides have (b) levels of structure which build in complexity to secondary and tertiary/quaternary structures and stem from the order of amino acids in the chain (the primary structure). Structure images were created using PEP-FOLD3 (https://bioserv.rpbs.univ-paris-diderot.fr/services/PEP-FOLD3) and the Protein Data Bank (PDB; http://www.rcsb.org/pdb/).

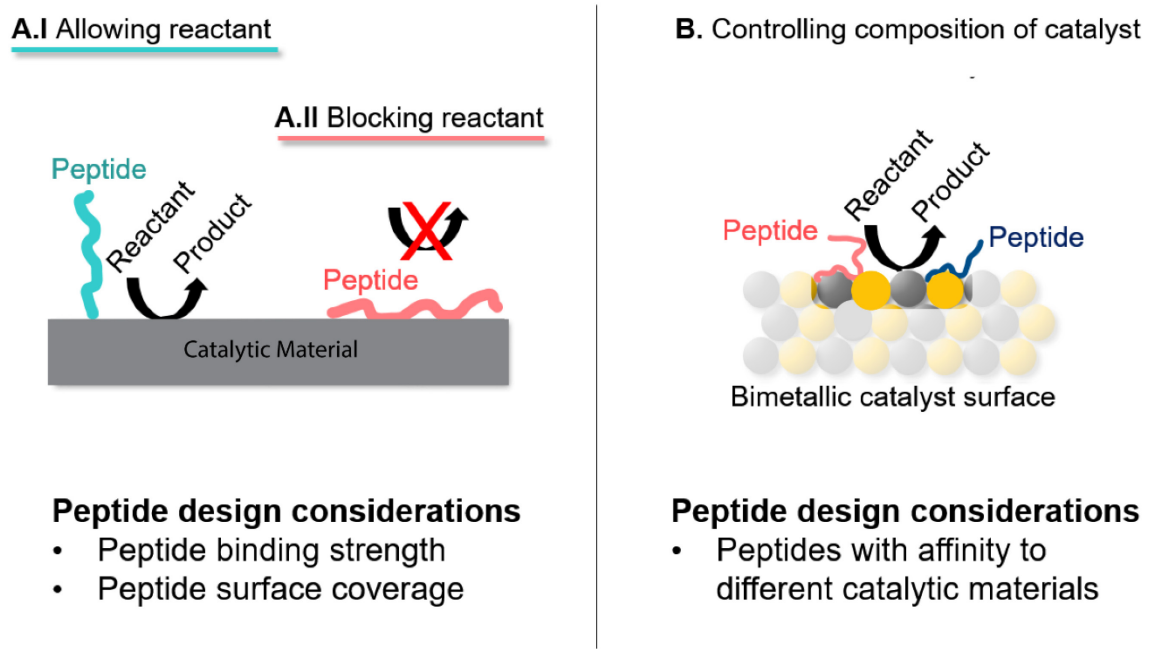


**Figure 3**: Surface-bound peptides can affect catalytic performance in two ways: (a) peptides can be designed with varying degrees of binding strength and surface coverage to modulate reactant exposure to the catalytic surface, and (b) amino acids and peptides can be designed to stabilize atoms on a surface and form different active catalytic compositions (e.g., bimetallic structures). Reproduced with pending permission from J. Electrochem. En. Conv. Stor. 2020, 17(4), 040801.

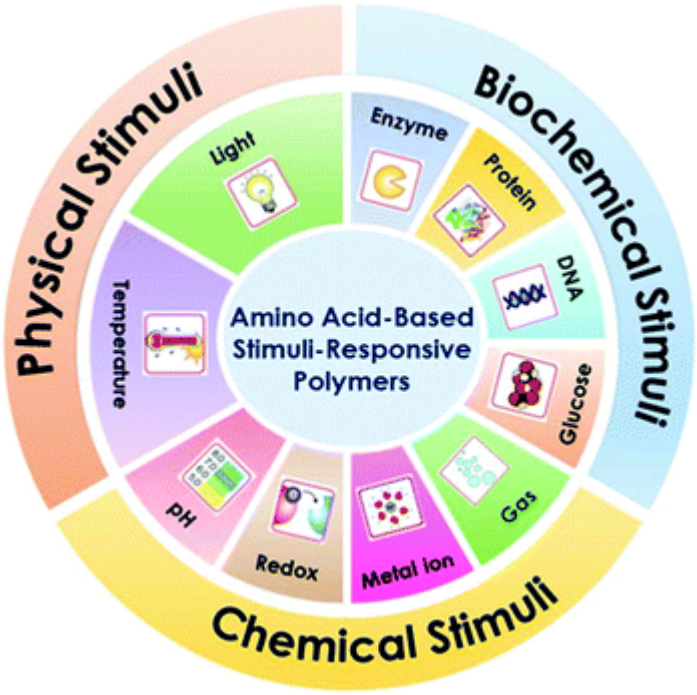


**Figure 4**: Polymers derived from amino acids have a variety of chemical, biochemical and physical stimuli. Reproduced with permission from Polym. Chem., 2018, 9, 1257-1287.[106]

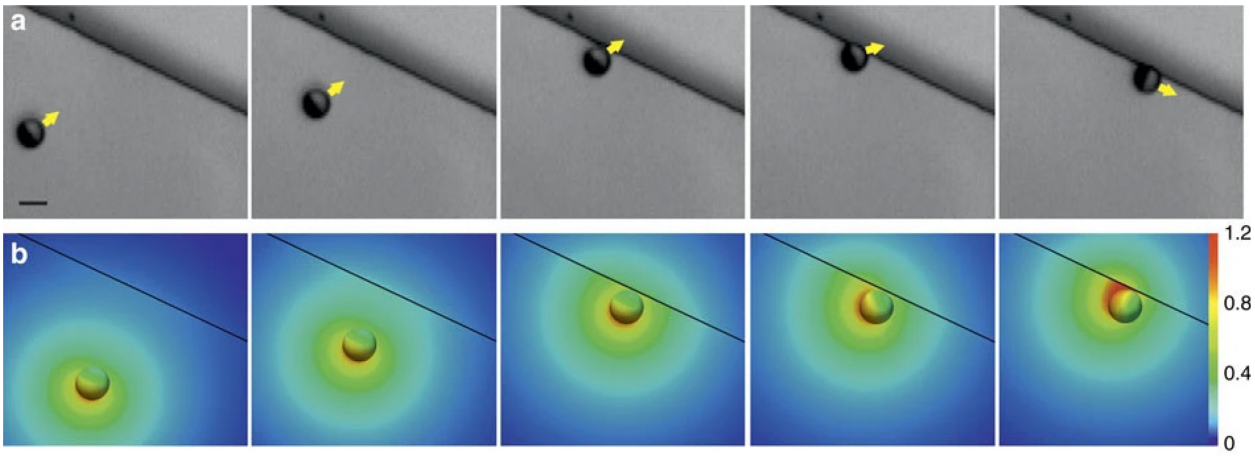


**Figure 5**: **Example of topography guides an active particle.** An (a) experimental view of a catalytic active Janus particle approaching a step and (b) a numerically calculated distribution of reaction products. The particle was 2.5 μm in radius, dispersed in 2.5% by volume hydrogen peroxide ($H_2O2$), and the step height was 800 nm. This work is an excellent example of how topography can guide the path of a catalytic active Janus particle. The scale bar is 5 μm. This figure was reproduced from an 'open access article distributed under the terms of the Creative Commons CC BY license, which permits unrestricted use, distribution, and reproduction in any medium, provided the original work is properly cited'.[117]

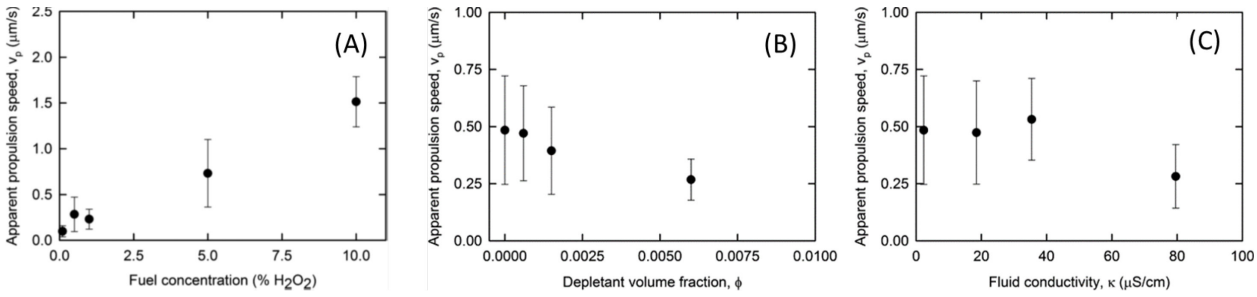


**Figure 6**: Apparent speed of Janus particles. The speed increased roughly linearly with increasing hydrogen peroxide concentration (A). The speed decreased as uncharged depletants volume fraction increased (B). Similarly, propulsion speed decreased at larger electrolyte conductivity. This figure was reproduced from an 'open access article published under an ACS AuthorChoice License, which permits copying and redistribution of the article or any adaptations for non-commercial purposes.[9]

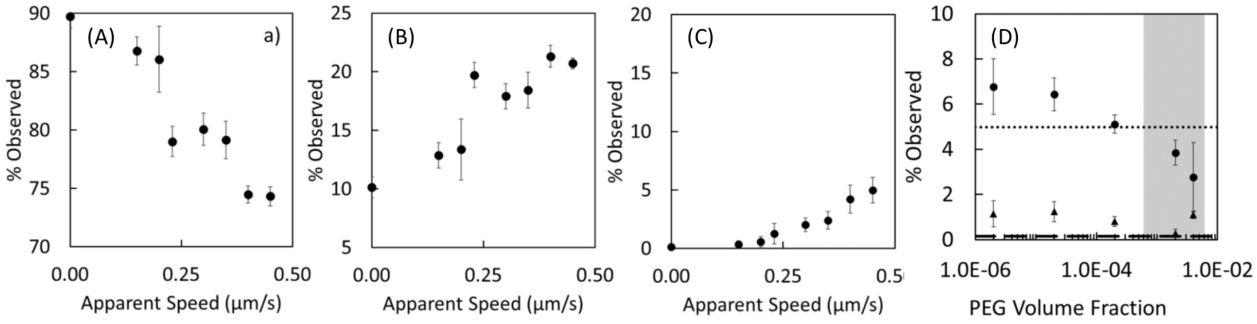


**Figure 7:** Mean extent of singlets (A) intermediate (B) and clusters (C). The rate of clustering represented by % Observed was enhanced by increasing peroxide concentrations. (D) Mean extent of clustering for active (3% $H_2O_2$) and passive (0% $H_2O_2$) because of PEG volume fraction. Clustering was enhanced for active particles (closed circles) at low PEG concentrations. This was not observed in passive (triangles) systems. Low PEG concentrations increased the attractive interactions between particles and enhanced cluster formation. Lastly, the broken line is the % Observed in the absence of both fuel and PEG. Reprinted from Colloids and Surfaces A: Physicochemical and Engineering Aspects, Vol. 627, Mohammed A. Kalil, Nicky R. Baumgartner, Marola W. Issa, Shawn D. Ryan, Christopher L. Wirth, Influence of PEG on the clustering of active Janus colloids, 127191, Copyright (2021), with permission from Elsevier.

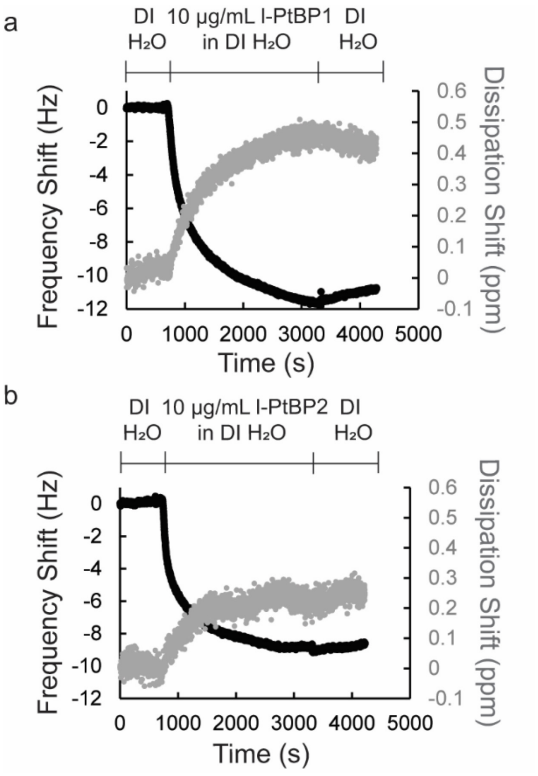


**Figure 8**: Time-course frequency shift (black) and dissipation shift (gray) data obtained via quartz crystal microbalance with dissipation monitoring for (a) l-PtBP1 and (b) l-PtBP2 adsorption to a platinum surface.

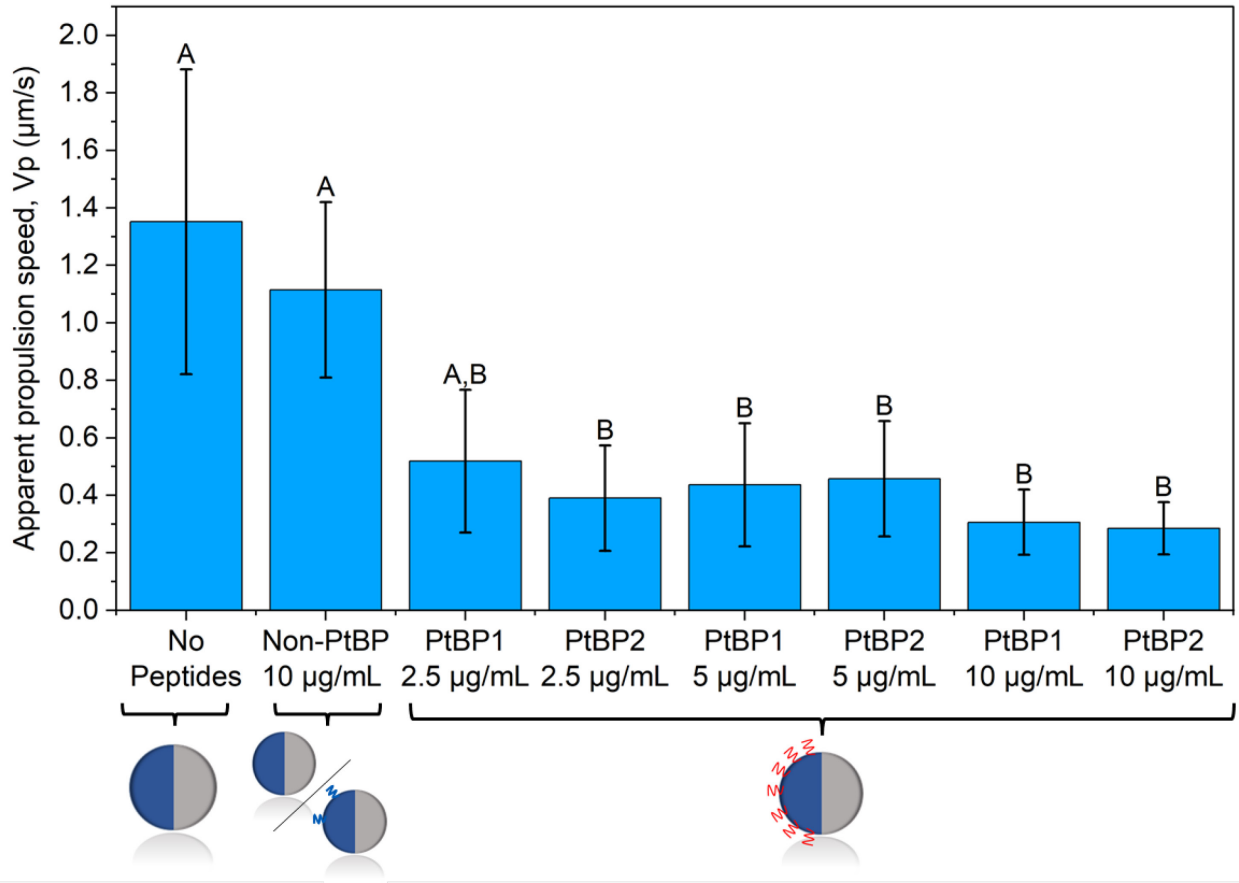


**Figure 9:** Apparent speed of Janus particles suspended in 3% hydrogen peroxide solutions. The speed was observed to significantly decrease for Janus particles functionalized with platinum-binding peptides. The various peptide concentrations used (2.5 µg/mL, 5 µg/mL, and 10 µg/mL) were all observed to quench the speed in a similar magnitude. This may be attributed to the effects of saturation where the effective surface coverage was reached at the smaller incubation concentrations. It is noted that PtBP1 incubated at 2.5 µg/mL was not significantly different from the control samples (no peptide and non-Pt binding peptide). The slight variations in particle size, inherent to our particle sample, will alter the propulsion speed and cause variation in the data. Columns not sharing a letter are significantly different according to a Dunn post-hoc test at a family α value of 0.025. Data are represented as the average +/- the standard deviation.

## AUTHOR INFORMATION

Corresponding Author

*Christopher L. Wirth

Department of Chemical and Biomolecular Engineering

Case School of Engineering

Case Western Reserve University

Cleveland, Ohio 44106, USA

wirth@case.edu

## AUTHOR CONTRIBUTIONS

The manuscript was written through contributions of all authors. All authors have given approval to the final version of the manuscript.

## FUNDING SOURCES

This work was supported by the National Science Foundation CAREER Award, NSF No. 2023525 (CLW) and National Science Foundation CAREER Award, NSF No. 2045033 (JNR).

REFERENCES


(1) Rashidi, A.; Issa, M. W.; Martin, I. T.; Avishai, A.; Razavi, S.; Wirth, C. L. Local Measurement of Janus Particle Cap Thickness. *ACS Appl. Mater. Interfaces* **2018**, *10*, 30925–30929.

(2) Walther, A.; Müller, A. H. E. Janus Particles. *Soft Matter* **2008**, *4*, 663.

(3) Jiang, H.; Hou, Z. Nonequilibrium Dynamics of Chemically Active Particles. *Chinese J. Chem.* **2022**, *40*, 419–429.

(4) Paxton, W. F.; Kistler, K. C.; Olmeda, C. C.; Sen, A.; St. Angelo, S. K.; Cao, Y.; Mallouk, T. E.; Lammert, P. E.; Crespi, V. H. Catalytic Nanomotors: Autonomous Movement of Striped Nanorods. *J. Am. Chem. Soc.* **2004**, *126*, 13424–13431.

(5) Wang, W.; Duan, W.; Ahmed, S.; Mallouk, T. E.; Sen, A. Small Power: Autonomous Nano- and Micromotors Propelled by Self-Generated Gradients. *Nano Today* **2013**, *8*, 531–534.

(6) Menzel, A. M. Tuned, Driven, and Active Soft Matter. *Phys. Rep.* **2015**, *554*, 1–45.

(7) Katuri, J.; Ma, X.; Stanton, M. M.; Sánchez, S. Designing Micro- and Nanoswimmers for Specific Applications. *Acc. Chem. Res.* **2017**, *50*, 2–11.

(8) Jiang, S.; Chen, Q.; Tripathy, M.; Luijten, E.; Schweizer, K. S.; Granick, S. Janus Particle Synthesis and Assembly. *Adv. Mater.* **2010**, *22*, 1060–1071.

(9) Issa, M. W. M. W.; Baumgartner, N. R. N. R.; Kalil, M. A. M. A.; Ryan, S. D. S. D.; Wirth, C. L. C. L. Charged Nanoparticles Quench the Propulsion of Active Janus Colloids. *ACS Omega* **2019**, *4*, 13034–13041.

(10) Kalil, M. A.; Baumgartner, N. R.; Issa, M. W.; Ryan, S. D.; Wirth, C. L. Influence of PEG on the Clustering of Active Janus Colloids. *Colloids Surfaces A Physicochem. Eng. Asp.* **2021**, *627*, 127191.

(11) Sharma, R.; Velev, O. D. Remote Steering of Self-Propelling Microcircuits by Modulated Electric Field. *Adv. Funct. Mater.* **2015**, *25*, 5512–5519.

(12) Chang, S. T.; Paunov, V. N.; Petsev, D. N.; Velev, O. D. Remotely Powered Self-Propelling Particles and Micropumps Based on Miniature Diodes. *Nat. Mater.* **2007**, *6*, 235–240.

(13) Dreyfus, R.; Baudry, J.; Roper, M. L.; Fermigier, M.; Stone, H. A.; Bibette, J. Microscopic Artificial Swimmers. *Nature* **2005**, *437*, 862–865.

(14) Tierno, P.; Golestanian, R.; Pagonabarraga, I.; Sagués, F. Magnetically Actuated Colloidal Microswimmers. *J. Phys. Chem. B* **2008**, *112*, 16525–16528.

(15) Tottori, S.; Zhang, L.; Peyer, K. E.; Nelson, B. J. Assembly, Disassembly, and Anomalous Propulsion of Microscopic Helices. *Nano Lett.* **2013**, *13*, 4263–4268.

(16) Anderson, J. L. Colloid Transport by Interfacial Forces. *Annu. Rev. Fluid Mech.* **1989**, *21*, 61–99.

(17) Schattling, P.; Thingholm, B.; Städler, B. Enhanced Diffusion of Glucose-Fueled Janus Particles. *Chem. Mater.* **2015**, *27*, 7412–7418.

(18) Wensink, H. H.; Löwen, H. Aggregation of Self-Propelled Colloidal Rods near Confining Walls. *Phys. Rev. E - Stat. Nonlinear, Soft Matter Phys.* **2008**, *78*, 20–23.

(19) Fily, Y.; Henkes, S.; Marchetti, M. C. Freezing and Phase Separation of Self-Propelled Disks. *Soft Matter* **2014**, *10*, 2132–2140.

(20) Ibrahim, Y.; Liverpool, T. B. The Dynamics of a Self-Phoretic Janus Swimmer near a Wall. *Eur. Lett.* **2015**, *111*, 48008.

(21) Ketzetzi, S.; de Graaf, J.; Doherty, R. P.; Kraft, D. J. Slip Length Dependent Propulsion Speed of Catalytic Colloidal Swimmers near Walls. *Phys. Rev. Lett.* **2020**, *124*, 048002.

(22) Volpe, G.; Buttinoni, I.; Vogt, D.; Kümmerer, H.-J.; Bechinger, C.; Kuemmerer, H.-J.;

Bechinger, C. Microswimmers in Patterned Environments. *Soft Matter* **2011**, *7*, 4.

(23) Patteson, A. E.; Gopinath, A.; Arratia, P. E. Active Colloids in Complex Fluids. *Curr. Opin. Colloid Interface Sci.* **2016**, *21*, 86–96.

(24) Ma, X.; Hahn, K.; Sanchez, S. Catalytic Mesoporous Janus Nanomotors for Active Cargo Delivery. *J. Am. Chem. Soc.* **2015**, *137*, 4976–4979.

(25) Baraban, L.; Tasinkevych, M.; Popescu, M. N.; Sanchez, S.; Dietrich, S.; Schmidt, O. G. Transport of Cargo by Catalytic Janus Micro-Motors. *Soft Matter* **2012**, *8*, 48–52.

(26) Servant, A.; Qiu, F.; Mazza, M.; Kostarelos, K.; Nelson, B. J. Controlled In Vivo Swimming of a Swarm of Bacteria-Like Microrobotic Flagella. *Adv. Mater.* **2015**, *27*, 2981–2988.

(27) Kaynak, M.; Ozcelik, A.; Nourhani, A.; Lammert, P. E.; Crespi, V. H.; Huang, T. J. Acoustic Actuation of Bioinspired Microswimmers. *Lab Chip* **2017**, *17*, 395–400.

(28) Bunea, A.-I.; Pavel, I.-A.; David, S.; Gáspár, S. Sensing Based on the Motion of Enzyme-Modified Nanorods. *Biosens. Bioelectron.* **2015**, *67*, 42–48.

(29) Leong, J. Y.; Tey, B. T.; Tan, C. P.; Chan, E. S. Nozzleless Fabrication of Oil-Core Biopolymeric Microcapsules by the Interfacial Gelation of Pickering Emulsion Templates. *ACS Appl. Mater. Interfaces* **2015**, *7*, 16169–16176.

(30) Partridge, J. D.; Ariel, G.; Schvartz, O.; Harshey, R. M.; Be'er, A. The 3D Architecture of a Bacterial Swarm Has Implications for Antibiotic Tolerance. *Sci. Rep.* **2018**, *8*, 15823.

(31) Sharan, P.; Xiao, Z.; Mancuso, V.; Uspal, W. E.; Simmchen, J. Upstream Rheotaxis of Catalytic Janus Spheres. *ACS Nano* **2022**, *16*, 4599–4608.

(32) Velegol, D.; Garg, A.; Guha, R.; Kar, A.; Kumar, M. Origins of Concentration Gradients for Diffusiophoresis. *Soft Matter* **2016**, *12*, 4686–4703.

(33) Howse, J. R.; Jones, R. A. L.; Ryan, A. J.; Gough, T.; Vafabakhsh, R.; Golestanian, R. Self-

Motile Colloidal Particles: From Directed Propulsion to Random Walk. *Phys. Rev. Lett.* **2007**, *99*, 8–11.

(34) Brown, A.; Poon, W. Ionic Effects in Self-Propelled Pt-Coated Janus Swimmers. *Soft Matter* **2014**, *10*, 4016.

(35) Brown, A. T.; Poon, W. C. K.; Holm, C.; de Graaf, J. Ionic Screening and Dissociation Are Crucial for Understanding Chemical Self-Propulsion in Polar Solvents. *Soft Matter* **2017**, *13*, 1200–1222.

(36) Ebbens, S.; Gregory, D. A.; Dunderdale, G.; Howse, J. R.; Ibrahim, Y.; Liverpool, T. B.; Golestanian, R. Electrokinetic Effects in Catalytic Pt-Insulator Janus Swimmers. *Eur. Lett.* **2014**, *106*, 58003.

(37) Lyu, X.; Liu, X.; Zhou, C.; Duan, S.; Xu, P.; Dai, J.; Chen, X.; Peng, Y.; Cui, D.; Tang, J.; et al. Active, Yet Little Mobility: Asymmetric Decomposition of H 2 O 2 Is Not Sufficient in Propelling Catalytic Micromotors. *J. Am. Chem. Soc.* **2021**, *143*, 12154–12164.

(38) Shields, C. W.; Velev, O. D. The Evolution of Active Particles: Toward Externally Powered Self-Propelling and Self-Reconfiguring Particle Systems. *Chem* **2017**, *3*, 539–559.

(39) Ma, F.; Yang, X.; Zhao, H.; Wu, N. Inducing Propulsion of Colloidal Dimers by Breaking the Symmetry in Electrohydrodynamic Flow. *Phys. Rev. Lett.* **2015**, *115*, 208302.

(40) Peng, X.; Chen, Z.; Kollipara, P. S.; Liu, Y.; Fang, J.; Lin, L.; Zheng, Y. Opto-Thermoelectric Microswimmers. *Light Sci. Appl.* **2020**, *9*, 141.

(41) Liu, M.; Zentgraf, T.; Liu, Y.; Bartal, G.; Zhang, X. Light-Driven Nanoscale Plasmonic Motors. *Nat. Nanotechnol.* **2010**, *5*, 570–573.

(42) Buttinoni, I.; Bialké, J.; Kümmel, F.; Löwen, H.; Bechinger, C.; Speck, T. Dynamical Clustering and Phase Separation in Suspensions of Self-Propelled Colloidal Particles. *Phys.*

*Rev. Lett.* **2013**, *110*, 238301.

(43) Shao, L.; Yang, Z.-J.; Andrén, D.; Johansson, P.; Käll, M. Gold Nanorod Rotary Motors Driven by Resonant Light Scattering. *ACS Nano* **2015**, *9*, 12542–12551.

(44) Jiang, H.-R.; Yoshinaga, N.; Sano, M. Active Motion of a Janus Particle by Self-Thermophoresis in a Defocused Laser Beam. *Phys. Rev. Lett.* **2010**, *105*, 268302.

(45) Zhang, L.; Zhang, H.; Liu, M.; Dong, B. Reprogrammable Logic Gate and Logic Circuit Based on Multistimuli-Responsive Raspberry-like Micromotors. *ACS Appl. Mater. Interfaces* **2016**, *8*, 15654–15660.

(46) Buttinoni, I.; Volpe, G.; Kümmel, F.; Volpe, G.; Bechinger, C. Active Brownian Motion Tunable by Light. *J. Phys. Condens. Matter* **2012**, *24*, 284129.

(47) Mair, L. O.; Evans, B. A.; Nacev, A.; Stepanov, P. Y.; Hilaman, R.; Chowdhury, S.; Jafari, S.; Wang, W.; Shapiro, B.; Weinberg, I. N. Magnetic Microkayaks: Propulsion of Microrods Precessing near a Surface by Kilohertz Frequency, Rotating Magnetic Fields. *Nanoscale* **2017**, *9*, 3375–3381.

(48) Ghosh, A.; Fischer, P. Controlled Propulsion of Artificial Magnetic Nanostructured Propellers. *Nano Lett.* **2009**, *9*, 2243–2245.

(49) Tottori, S.; Zhang, L.; Qiu, F.; Krawczyk, K. K.; Franco-Obregón, A.; Nelson, B. J. Magnetic Helical Micromachines: Fabrication, Controlled Swimming, and Cargo Transport. *Adv. Mater.* **2012**, *24*, 811–816.

(50) SQUIRES, T. M.; BAZANT, M. Z. Induced-Charge Electro-Osmosis. *J. Fluid Mech.* **2004**, *509*, 217–252.

(51) Harraq, A. Al; Choudhury, B. D.; Bharti, B. Field-Induced Assembly and Propulsion of Colloids. *Langmuir* **2022**, *38*, 3001–3016.

(52) Spatafora-Salazar, A.; Lobmeyer, D. M.; Cunha, L. H. P.; Joshi, K.; Biswal, S. L. Hierarchical Assemblies of Superparamagnetic Colloids in Time-Varying Magnetic Fields. *Soft Matter* **2021**, *17*, 1120–1155.

(53) Han, K.; Shields, C. W.; Velev, O. D. Engineering of Self-Propelling Microbots and Microdevices Powered by Magnetic and Electric Fields. *Adv. Funct. Mater.* **2018**, *28*, 1705953.

(54) Koleoso, M.; Feng, X.; Xue, Y.; Li, Q.; Munshi, T.; Chen, X. Micro/Nanoscale Magnetic Robots for Biomedical Applications. *Mater. Today Bio* **2020**, *8*, 100085.

(55) Ji, Y.; Lin, X.; Zhang, H.; Wu, Y.; Li, J.; He, Q. Thermoresponsive Polymer Brush Modulation on the Direction of Motion of Phoretically Driven Janus Micromotors. *Angew. Chemie Int. Ed.* **2019**, *58*, 4184–4188.

(56) Heidari, M.; Bregulla, A.; Landin, S. M.; Cichos, F.; von Klitzing, R. Self-Propulsion of Janus Particles near a Brush-Functionalized Substrate. *Langmuir* **2020**, *36*, 7775–7780.

(57) Zhang, P.; Li, M.; Xiao, C.; Chen, X. Stimuli-Responsive Polypeptides for Controlled Drug Delivery. *Chem. Commun.* **2021**, *57*, 9489–9503.

(58) Wang, Y.; Hernandez, R. M.; Bartlett, D. J.; Bingham, J. M.; Kline, T. R.; Sen, A.; Mallouk, T. E. Bipolar Electrochemical Mechanism for the Propulsion of Catalytic Nanomotors in Hydrogen Peroxide Solutions. *Langmuir* **2006**, *22*, 10451–10456.

(59) Wang, W.; Mallouk, T. E. A Practical Guide to Analyzing and Reporting the Movement of Nanoscale Swimmers. *ACS Nano* **2021**, *15*, 15446–15460.

(60) Al Harraq, A.; Bello, M.; Bharti, B. A Guide to Design the Trajectory of Active Particles: From Fundamentals to Applications. *Curr. Opin. Colloid Interface Sci.* **2022**, *61*, 101612.

(61) Palacci, J.; Sacanna, S.; Steinberg, A. P.; Pine, D. J.; Chaikin, P. M. Living Crystals of

Light-Activated Colloidal Surfers. *Science (80-. ).* **2013**, *339*, 936–940.

(62) Prieve, D. C. Measurement of Colloidal Forces with TIRM. *Adv. Colloid Interface Sci.* **1999**, *82*, 93–125.

(63) Swavola, J. C.; Edwards, T. D.; Bevan, M. A. Direct Measurement of Macromolecule-Coated Colloid-Mucus Interactions. *Langmuir* **2015**, *31*, 9076–9085.

(64) Bevan, M. A.; Prieve, D. C. Forces and Hydrodynamic Interactions between Polystyrene Surfaces with Adsorbed PEO−PPO−PEO. *Langmuir* **2000**, *16*, 9274–9281.

(65) Biggs, S.; Prieve, D. C.; Dagastine, R. R. Direct Comparison of Atomic Force Microscopic and Total Internal Reflection Microscopic Measurements in the Presence of Nonadsorbing Polyelectrolytes. *Langmuir* **2005**, *21*, 5421–5428.

(66) Biggs, S.; Dagastine, R. R.; Prieve, D. C. Oscillatory Packing and Depletion of Polyelectrolyte Molecules at an Oxide−Water Interface. *J. Phys. Chem. B* **2002**, *106*, 11557–11564.

(67) Bechinger, C.; Di Leonardo, R.; Löwen, H.; Reichhardt, C.; Volpe, G.; Volpe, G. Active Particles in Complex and Crowded Environments. *Rev. Mod. Phys.* **2016**, *88*, 045006.

(68) Uspal, W. E.; Popescu, M. N.; Dietrich, S.; Tasinkevych, M. Self-Propulsion of a Catalytically Active Particle near a Planar Wall: From Reflection to Sliding and Hovering. *Soft Matter* **2015**, *11*, 434–438.

(69) Wang, M. Effect of Boundaries on Noninteracting Weakly Active Particles in Different Geometries. *Phys. Rev. E* **2021**, *103*, 042609.

(70) Das, S.; Garg, A.; Campbell, A. I.; Howse, J.; Sen, A.; Velegol, D.; Golestanian, R.; Ebbens, S. J. Boundaries Can Steer Active Janus Spheres. *Nat. Commun.* **2015**, *6*, 8999.

(71) Wang, Y.; Katyal, P.; Montclare, J. K. Protein-Engineered Functional Materials. *Adv.*

*Healthc. Mater.* **2019**, *8*, 1801374.

(72) Karavasili, C.; Fatouros, D. G. Self-Assembling Peptides as Vectors for Local Drug Delivery and Tissue Engineering Applications. *Adv. Drug Deliv. Rev.* **2021**, *174*, 387–405.

(73) Varanko, A.; Saha, S.; Chilkoti, A. Recent Trends in Protein and Peptide-Based Biomaterials for Advanced Drug Delivery. *Adv. Drug Deliv. Rev.* **2020**, *156*, 133–187.

(74) Rondon, A.; Mahri, S.; Morales-Yanez, F.; Dumoulin, M.; Vanbever, R. Protein Engineering Strategies for Improved Pharmacokinetics. *Adv. Funct. Mater.* **2021**, *31*, 2101633.

(75) Jiang, Y.; Chen, Y.; Song, Z.; Tan, Z.; Cheng, J. Recent Advances in Design of Antimicrobial Peptides and Polypeptides toward Clinical Translation. *Adv. Drug Deliv. Rev.* **2021**, *170*, 261–280.

(76) Katyal, P.; Meleties, M.; Montclare, J. K. Self-Assembled Protein- and Peptide-Based Nanomaterials. *ACS Biomater. Sci. Eng.* **2019**, *5*, 4132–4147.

(77) Ahn, W.; Lee, J.-H.; Kim, S. R.; Lee, J.; Lee, E. J. Designed Protein- and Peptide-Based Hydrogels for Biomedical Sciences. *J. Mater. Chem. B* **2021**, *9*, 1919–1940.

(78) Wang, Y.; Zhang, W.; Gong, C.; Liu, B.; Li, Y.; Wang, L.; Su, Z.; Wei, G. Recent Advances in the Fabrication, Functionalization, and Bioapplications of Peptide Hydrogels. *Soft Matter* **2020**, *16*, 10029–10045.

(79) Renner, J. N.; Minteer, S. D. The Use of Engineered Protein Materials in Electrochemical Devices. *Exp. Biol. Med.* **2016**, *241*, 980–985.

(80) Adamson, H.; Jeuken, L. J. C. Engineering Protein Switches for Rapid Diagnostic Tests. *ACS Sensors* **2020**, *5*, 3001–3012.

(81) Bilal, M.; Iqbal, H. M. N. Tailoring Multipurpose Biocatalysts via Protein Engineering

Approaches: A Review. *Catal. Letters* **2019**, *149*, 2204–2217.

(82) Liu, Q.; Xun, G.; Feng, Y. The State-of-the-Art Strategies of Protein Engineering for Enzyme Stabilization. *Biotechnol. Adv.* **2019**, *37*, 530–537.

(83) Misra, R.; Rudnick-Glick, S.; Adler-Abramovich, L. From Folding to Assembly: Functional Supramolecular Architectures of Peptides Comprised of Non-Canonical Amino Acids. *Macromol. Biosci.* **2021**, *21*, 2100090.

(84) Won, Y.; Pagar, A. D.; Patil, M. D.; Dawson, P. E.; Yun, H. Recent Advances in Enzyme Engineering through Incorporation of Unnatural Amino Acids. *Biotechnol. Bioprocess Eng.* **2019**, *24*, 592–604.

(85) DiMarco, R. L.; Heilshorn, S. C. Multifunctional Materials through Modular Protein Engineering. *Adv. Mater.* **2012**, *24*, 3923–3940.

(86) Puetz, J.; Wurm, F. M. Recombinant Proteins for Industrial versus Pharmaceutical Purposes: A Review of Process and Pricing. *Processes* **2019**, *7*, 476.

(87) Pennington, M. W.; Zell, B.; Bai, C. J. Commercial Manufacturing of Current Good Manufacturing Practice Peptides Spanning the Gamut from Neoantigen to Commercial Large-Scale Products. *Med. Drug Discov.* **2021**, *9*, 100071.

(88) Packer, M. S.; Liu, D. R. Methods for the Directed Evolution of Proteins. *Nat. Rev. Genet.* **2015**, *16*, 379–394.

(89) Arnold, F. H. Directed Evolution: Bringing New Chemistry to Life. *Angew. Chemie Int. Ed.* **2018**, *57*, 4143–4148.

(90) Korendovych, I. V. Rational and Semirational Protein Design; 2018; pp 15–23.

(91) Huang, P.-S.; Boyken, S. E.; Baker, D. The Coming of Age of de Novo Protein Design. *Nature* **2016**, *537*, 320–327.

(92) Sequeiros-Borja, C. E.; Surpeta, B.; Brezovsky, J. Recent Advances in User-Friendly Computational Tools to Engineer Protein Function. *Brief. Bioinform.* **2021**, *22*.

(93) Xu, Y.; Verma, D.; Sheridan, R. P.; Liaw, A.; Ma, J.; Marshall, N. M.; McIntosh, J.; Sherer, E. C.; Svetnik, V.; Johnston, J. M. Deep Dive into Machine Learning Models for Protein Engineering. *J. Chem. Inf. Model.* **2020**, *60*, 2773–2790.

(94) Lin, C.-Y.; Liu, J. C. Modular Protein Domains: An Engineering Approach toward Functional Biomaterials. *Curr. Opin. Biotechnol.* **2016**, *40*, 56–63.

(95) Jiang, Z.; Guan, J.; Qian, J.; Zhan, C. Peptide Ligand-Mediated Targeted Drug Delivery of Nanomedicines. *Biomater. Sci.* **2019**, *7*, 461–471.

(96) Chiu, C.-Y.; Ruan, L.; Huang, Y. Biomolecular Specificity Controlled Nanomaterial Synthesis. *Chem. Soc. Rev.* **2013**, *42*, 2512–2527.

(97) Sfragano, P. S.; Moro, G.; Polo, F.; Palchetti, I. The Role of Peptides in the Design of Electrochemical Biosensors for Clinical Diagnostics. *Biosensors* **2021**, *11*, 246.

(98) Mahmoudi Gomari, M.; Saraygord-Afshari, N.; Farsimadan, M.; Rostami, N.; Aghamiri, S.; Farajollahi, M. M. Opportunities and Challenges of the Tag-Assisted Protein Purification Techniques: Applications in the Pharmaceutical Industry. *Biotechnol. Adv.* **2020**, *45*, 107653.

(99) Gupta, S.; Azadvari, N.; Hosseinzadeh, P. Design of Protein Segments and Peptides for Binding to Protein Targets. *BioDesign Res.* **2022**, *2022*, 1–25.

(100) Seker, U. O. S.; Demir, H. V. Material Binding Peptides for Nanotechnology. *Molecules* **2011**, *16*, 1426–1451.

(101) Pramounmat, N.; Yan, K.; Wolf, J.; Renner, J. Platinum-Binding Peptides: Understanding of Selective Binding and Multifunctionality. *Multifunct. Mater.* **2022**.

(102) Zong, J.; Cobb, S. L.; Cameron, N. R. Peptide-Functionalized Gold Nanoparticles: Versatile Biomaterials for Diagnostic and Therapeutic Applications. *Biomater. Sci.* **2017**, *5*, 872–886.

(103) Loney, C. N.; Maheshwari, S.; Pramounmat, N.; Janik, M. J.; Renner, J. N. Effects of Peptide-Functionalized Surfaces on the Electrochemical Hydrogen Evolution Reaction. *J. Electrochem. Energy Convers. Storage* **2020**, *17*.

(104) Walsh, T. R.; Knecht, M. R. Biointerface Structural Effects on the Properties and Applications of Bioinspired Peptide-Based Nanomaterials. *Chem. Rev.* **2017**, *117*, 12641–12704.

(105) Bedford, N. M.; Hughes, Z. E.; Tang, Z.; Li, Y.; Briggs, B. D.; Ren, Y.; Swihart, M. T.; Petkov, V. G.; Naik, R. R.; Knecht, M. R.; et al. Sequence-Dependent Structure/Function Relationships of Catalytic Peptide-Enabled Gold Nanoparticles Generated under Ambient Synthetic Conditions. *J. Am. Chem. Soc.* **2016**, *138*, 540–548.

(106) Bauri, K.; Nandi, M.; De, P. Amino Acid-Derived Stimuli-Responsive Polymers and Their Applications. *Polym. Chem.* **2018**, *9*, 1257–1287.

(107) Shen, Y.; Fu, X.; Fu, W.; Li, Z. Biodegradable Stimuli-Responsive Polypeptide Materials Prepared by Ring Opening Polymerization. *Chem. Soc. Rev.* **2015**, *44*, 612–622.

(108) Huang, J.; Heise, A. Stimuli Responsive Synthetic Polypeptides Derived from N-Carboxyanhydride (NCA) Polymerisation. *Chem. Soc. Rev.* **2013**, *42*, 7373.

(109) Varanko, A. K.; Su, J. C.; Chilkoti, A. Elastin-Like Polypeptides for Biomedical Applications. *Annu. Rev. Biomed. Eng.* **2020**, *22*, 343–369.

(110) Oliva, N.; Almquist, B. D. Spatiotemporal Delivery of Bioactive Molecules for Wound Healing Using Stimuli-Responsive Biomaterials. *Adv. Drug Deliv. Rev.* **2020**, *161–162*, 22–41.

(111) Song, Y.; Ding, Y.; Dong, C. <scp>Stimuli-responsive</Scp> Polypeptide Nanoassemblies: Recent Progress and Applications in Cancer Nanomedicine. *WIREs Nanomedicine and Nanobiotechnology* **2022**, *14*.

(112) Lawrence, R. L.; Scola, B.; Li, Y.; Lim, C.-K.; Liu, Y.; Prasad, P. N.; Swihart, M. T.; Knecht, M. R. Remote Optically Controlled Modulation of Catalytic Properties of Nanoparticles through Reconfiguration of the Inorganic/Organic Interface. *ACS Nano* **2016**, *10*, 9470–9477.

(113) Lawrence, R. L.; Hughes, Z. E.; Cendan, V. J.; Liu, Y.; Lim, C.-K.; Prasad, P. N.; Swihart, M. T.; Walsh, T. R.; Knecht, M. R. Optical Control of Nanoparticle Catalysis Influenced by Photoswitch Positioning in Hybrid Peptide Capping Ligands. *ACS Appl. Mater. Interfaces* **2018**, *10*, 33640–33651.

(114) Olagunju, M. O.; Liu, Y.; Frenkel, A. I.; Knecht, M. R. Atomically Resolved Characterization of Optically Driven Ligand Reconfiguration on Nanoparticle Catalyst Surfaces. *ACS Appl. Mater. Interfaces* **2021**, *13*, 44302–44311.

(115) Lawrence, R. L.; Olagunju, M. O.; Liu, Y.; Mahalingam, K.; Slocik, J. M.; Naik, R. R.; Frenkel, A. I.; Knecht, M. R. Remote Controlled Optical Manipulation of Bimetallic Nanoparticle Catalysts Using Peptides. *Catal. Sci. Technol.* **2021**, *11*, 2386–2395.

(116) Tuson, H. H.; Weibel, D. B. Bacteria–Surface Interactions. *Soft Matter* **2013**, *9*, 4368.

(117) Simmchen, J.; Katuri, J.; Uspal, W. E.; Popescu, M. N.; Tasinkevych, M.; Sánchez, S. Topographical Pathways Guide Chemical Microswimmers. *Nat. Commun.* **2016**, *7*, 10598.

(118) Brown, A. T.; Vladescu, I. D.; Dawson, A.; Vissers, T.; Schwarz-Linek, J.; Lintuvuori, J. S.; Poon, W. C. K. Swimming in a Crystal. *Soft Matter* **2016**, *12*, 131–140.

(119) Ketzetzi, S.; Rinaldin, M.; Dröge, P.; Graaf, J. de; Kraft, D. J. Activity-Induced Interactions

and Cooperation of Artificial Microswimmers in One-Dimensional Environments. *Nat. Commun.* **2022**, *13*, 1772.

(120) McGlasson, A.; Bradley, L. C. Investigating Time-Dependent Active Motion of Janus Micromotors Using Dynamic Light Scattering. *Small* **2021**, *17*, 2104926.

(121) Crocker, J. C.; Grier, D. G. Methods of Digital Video Microscopy for Colloidal Studies. *J. Colloid Interface Sci.* **1996**, *179*, 298–310.

(122) Grier, D. G. GitHub repository for particle tracking code https://github.com/davidgrier/features/.

(123) Seker, U. O. S.; Wilson, B.; Sahin, D.; Tamerler, C.; Sarikaya, M. Quantitative Affinity of Genetically Engineered Repeating Polypeptides to Inorganic Surfaces. *Biomacromolecules* **2009**, *10*, 250–257.

(124) Pramounmat, N.; Loney, C. N.; Kim, C.; Wiles, L.; Ayers, K. E.; Kusoglu, A.; Renner, J. N. Controlling the Distribution of Perfluorinated Sulfonic Acid Ionomer with Elastin-like Polypeptide. *ACS Appl. Mater. Interfaces* **2019**, *11*, 43649–43658.

(125) Su, Z.; Pramounmat, N.; Watson, S. T.; Renner, J. N. Engineered Interaction between Short Elastin-like Peptides and Perfluorinated Sulfonic-Acid Ionomer. *Soft Matter* **2018**, *14*, 3528–3535.

(126) Sauerbrey, Gjz. Use of Quartz Vibrator for Weighting Thin Films on a Microbalance. *Zeitschrift fur Phys.* **1959**, *155*, 206–212.

(127) Ussia, M.; Pumera, M. Towards Micromachine Intelligence: Potential of Polymers. *Chem. Soc. Rev.* **2022**, *51*, 1558–1572.

(128) Chen, C.; Tang, S.; Teymourian, H.; Karshalev, E.; Zhang, F.; Li, J.; Mou, F.; Liang, Y.; Guan, J.; Wang, J. Chemical/Light-Powered Hybrid Micromotors with “On-the-Fly”

Optical Brakes. *Angew. Chemie Int. Ed.* **2018**, *57*, 8110–8114.

(129) Vutukuri, H. R.; Lisicki, M.; Lauga, E.; Vermant, J. Light-Switchable Propulsion of Active Particles with Reversible Interactions. *Nat. Commun.* **2020**, *11*, 2628.

(130) Reviakine, I.; Johannsmann, D.; Richter, R. P. Hearing What You Cannot See and Visualizing What You Hear: Interpreting Quartz Crystal Microbalance Data from Solvated Interfaces. *Anal. Chem.* **2011**, *83*, 8838–8848.

(131) Su, Z.; Kole, S.; Harden, L. C.; Palakkal, V. M.; Kim, C.; Nair, G.; Arges, C. G.; Renner, J. N. Peptide-Modified Electrode Surfaces for Promoting Anion Exchange Ionomer Microphase Separation and Ionic Conductivity. *ACS Mater. Lett.* **2019**, *1*, 467–475.

(132) Pramounmat, N.; Asaei, S.; Hostert, J. D.; Young, K.; von Recum, H. A.; Renner, J. N. Grafting of Short Elastin-like Peptides Using an Electric Field. *Sci. Rep.* **2022**, *12*, 18682.

(133) Seker, U. O. S.; Wilson, B.; Dincer, S.; Kim, I. W.; Oren, E. E.; Evans, J. S.; Tamerler, C.; Sarikaya, M. Adsorption Behavior of Linear and Cyclic Genetically Engineered Platinum Binding Peptides. *Langmuir* **2007**, *23*, 7895–7900.

(134) Dinçer, S.; Tamerler, C.; Sarıkaya, M.; Pişkin, E. Photoresponsive Peptide–Azobenzene Conjugates That Specifically Interact with Platinum Surfaces. *Surf. Sci.* **2008**, *602*, 1757–1762.